COMPARISON OF CONTROL LAWS FOR MAGNETIC LEVITATION

Yoichi KANEMITSU **Masaru OHSAWA** **Eishi MARUI**
EBARA RESEARCH CO. LTD
2-1 Hon-Fujisawa 4-chome, Fujisawa-shi, Kanagawa ,JAPAN

ABSTRACT

We have compared and evaluated the performances of the various control theories (LQG, H∞, TDC, Sliding Mode Control and PID) to control a test apparatus levitating a flexible body by electromagnetic force. The test apparatus is a system controlling magnetic pull in the same way as magnetic bearing and magnetic levitation system. The aspects compared are : disturbance suppression effect, robustness, stability, response speed, rigidity, and steady-state characteristic.

INTRODUCTION

In recent years, several instances of the application of new control theories to magnetic bearings and levitation systems have been reported. However, there have been no reports comparing these various control theories. In the present research, we have compared and evaluated the performances of the various control theories (LQG[2], H∞[3], TDC[5], Sliding Mode Control[4] and PID[1]) to control a test apparatus levitating a flexible body by electromagnetic force. The test apparatus is a system controlling magnetic pull in the same way as magnetic bearing and magnetic levitation system. The aspects compared are disturbance suppression effect, robustness, stability, response speed, rigidity, and steady-state characteristic. If magnetic bearings and magnetic levitation system are used for levitation control, distortion vibration of the levitating body is a problem. In this research the levitating body was connected between 2 partial spheres and a ring, by means of 2 sets of diaphragms. Consequently, the levitating body has two distortion vibration modes, resulting from the distortion of the diaphragms.

EXPERIMENT APPARATUS

The experiment apparatus used in this research is shown in Fig. 1. The apparatus was constructed from a gap sensor, a controller (DSP), power amplifier,magnetizing coil, and levitating body.

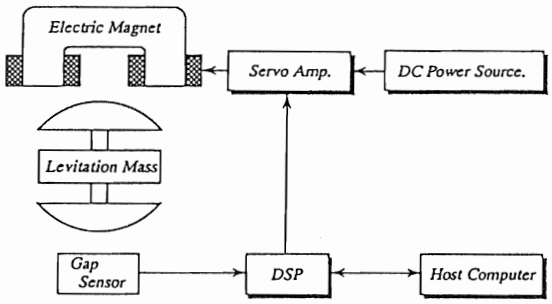

FIGURE 1: Construction of Electromagnetic Levitation System

A non-contacting eddy current displacement sensor was used to measure the position of the lower surface of the partial sphere under the levitating body. Sensor gain was 67V/m. DSP was used to implement the required controller, in accordance with the control theory being evaluated. The controller program was rewritten as a program for DSP control, and this was downloaded from the host computer to a DSP board. The sampling frequency of the analog-to-digital and digital-to-analog converters fitted on the DSP board was 20kHz. The plant model consists of control coil and levitating body. To avoid the power amplifier characteristics of the magnetizung coil affecting the results when the tests were carried out, an amplifier with gain 1 and almost flat frequency characteristics of from DC to 500Hz was used.

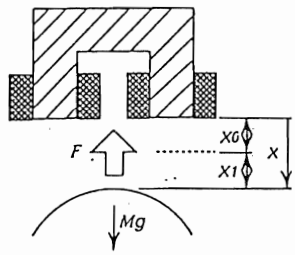

FIGURE 2: Electromagnetic Forces Acting on Levitation System

As shown in Fig. 2, when the force produced by the magnetizing coil is F, the equation for the motion of the levitated body is:

$$M\frac{d^2x}{dt^2} = Mg - F \tag{1}$$

where M: Mass of levitating body, F: Magnetic pull , x: Gap between magnet pole and levitating body , g: Gravitational acceleration
Using coil inductance L and applied current i, equation (1) can be written as:

$$M\frac{d^2x}{dt^2} = Mg + \frac{1}{2}i^2\frac{\partial L(x)}{\partial x} \tag{2}$$

Assuming coil inductance to be:

$$L = \frac{L_o}{1 + x/a}L_{oo} \tag{3}$$

(a, L_0 and L_{00} are constants obtained from an identification test under the condition assumed above), then

$$x = x_o + x_1 \tag{4}$$

$$i = i_o + i_1 \tag{5}$$

where, x_0: Balance position, i_0: Applied current at balance position
Linearizing in the region of the balance point, we obtain:

$$\frac{1}{2}i^2\frac{\partial L}{\partial x} = -\frac{aL_o}{2(a+x_o)^2}(i_o^2 + 2i_oi_1 - \frac{2i_o^2}{a+x_o}x_1) \tag{6}$$

Furthermore, in the balanced state:

$$Mg = \frac{aL_o}{2(a+x_o)^2}i_o^2 \tag{7}$$

and consequently (2) becomes:

$$M\frac{d^2x}{dt^2} = -\frac{aL_oi_o}{(a+x_o)^2}i_1 + \frac{aL_oi_o^2}{(a+x_o)^3}x_1 \tag{8}$$

Finally, by transforming (8), we obtain the following state equations:

$$\dot{\mathbf{x}} = \mathbf{Ax} + \mathbf{Bu}$$
$$\mathbf{y} = \mathbf{cx} \tag{9}$$

where:

$$\mathbf{x} = \begin{bmatrix} x_1 \\ x_2 \end{bmatrix}, u = i_1, x_2 = \dot{x}_1$$

$$\mathbf{A} = \begin{bmatrix} 0 & 1 \\ \alpha & 0 \end{bmatrix}, \mathbf{B} = \begin{bmatrix} 0 \\ \beta \end{bmatrix}, \mathbf{c} = [1 \quad 0]$$

$$\alpha = \frac{L_oi_o^2}{Ma^2(1+x_o/a)^2} = -2614.65$$

$$\beta = -\frac{L_oi_o^2}{Ma(1+x_o/a)^2} = -8.73$$

The frequency characteristics of the control object are shown in Fig.3.

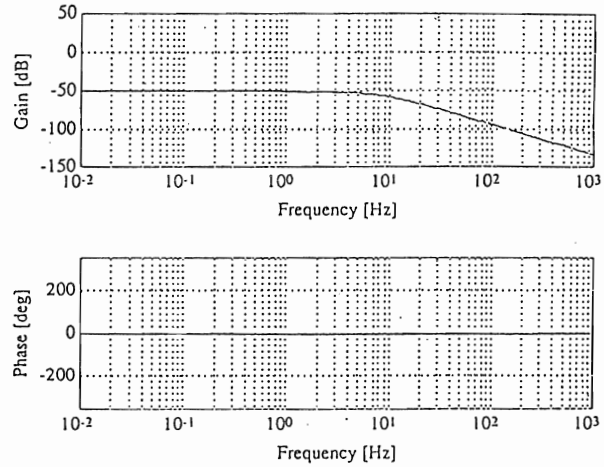

FIGURE 3: Bode Plot of Plant (elastic vibration of the levitating body is disregarded).

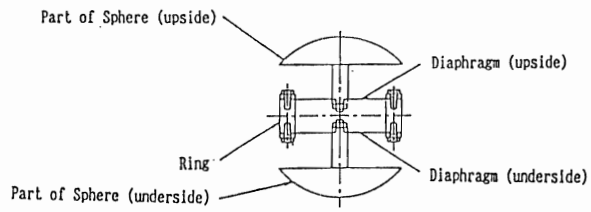

FIGURE 4: Structure of Levitated Body

The construction of the levitating body is as shown in Fig.4. When the number of diaphragms is changed, the vibration characteristics of the control object also change. As shown in Fig.5, the transfer function measured for the levitating body has the characteristic of having two peaks, due to the distortion vibration mode. However, in the plant model used in this research, a distortion vibration mode was not included, and this effect was considered to be spillover proving the robustness of the controller. Because this measurement value includes sensor gain, it is 56.3dB higher than the frequency characteristic gain obtained by calculation.

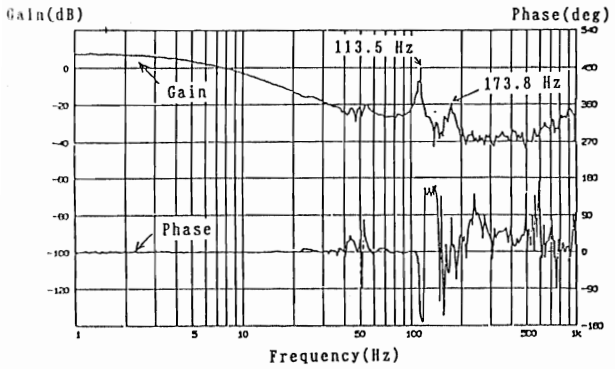

FIGURE 5: Bode Diagram of Plant(In case using diaphragms by ones at top and bottom)

CONTROLLERS OBTAINED USING THE DIFFERENT CONTROL THEORIES

PID Control For the PID theory, a controller was constructed that combines proportional, integral and differential elements to stabilize the system. In accordance with the stabilization theory of classical control, stability is judged by calculating the open loop characteristics of the system and using the gain margin and phase margin values obtained. The controller used in this research utilizes incomplete integrals and incomplete differentials to improve the dynamic characteristics of the system. The elements are arranged in series to facilitate calculation. The following 3 design guidelines were employed:

1. Stability of the system (stable levitation)
2. Raise gain (DC gain) at low frequency to improve steady-state characteristics.
3. Decrease gain in high frequency range to suppress vibration in distortion vibration mode.

As a result, the following transfer functions were obtained for the each element:
Proportional element $Kp = 0.2$
Integral element $Ci(s) = (s + 62.832)/(s + 6.2832)$
Differential element $Cd(s) = 10(s + 12.566)/(s + 125.66)$

Controller $C(s)$ is defined by these elements, according to the following eguation.

$$C(s) = K_p \cdot C_1(s) \cdot C_d(s) \tag{10}$$

LQG Control For the LQG theory, a regulator optimally suited to a linear control object was constructed, using the quadratic form of the evaluation function. In addition, it was assumed that disturbance and sensor noise would be random signals with Gaussian distribution, and an optimal filter was constructed that can measure the state even when such noises are present. That is, the intention was to construct a statistically optimal feedback system by using an optimal regulator and an optimal filter (Karman filter). The design guidelines for the LQG control were:

1. Trade-off between responsibility and stability on the one hand, and control input on the other hand.
2. Countermeasures for disturbance in the high frequency range, to suppress vibration caused by spillover.

The feedback gain matrix of the controller constructed according to the above guidelines is:

$$\begin{bmatrix} -102.26 & 1.000 & 102.26 \\ -7857.0 & -224.53 & 5228.3 \\ -600.36 & -33.727 & 0.0000 \end{bmatrix} \tag{11}$$

$H\infty$ Contrpl Modern control , represented by LQG , requires that data regarding the control object must be correctly ascertained. However, "uncertainty" arises when the control object is modelled in actual fact. In classical control this "uncertainty" was dealt with by treating it as phase margin or gain margin, but in modern control this "uncertainty" is problematic. However, with $H\infty$ control by utilizing $H\infty$ norm, not only can the conventional system-stabilizing design be retained, but also, the error caused by disturbance and "uncertainty" of the model can be controlled. The guidelines for design using the $H\infty$ theory were;

1. Use frequency-domain weight function relative to sensitivity function to suppress disturbance in the low frequency range.
2. Use frequency-domain weight function relative to complementary sensitivity function to suppress "uncertainty " caused by spillover.

Accordingly, the weight function relative to the sensitivity function, W_s, is

$$W_s = 5\frac{0.1 \times 2\pi}{s + 0.1 \times 2\pi} \tag{12}$$

and the weight function relative to the complementary sensitivity function W_t, is

$$W_t = \frac{1}{10000}\frac{(s + 0.5 \times 2\pi)(s + 20 \times 2\pi)}{0.5 \times 20 \times 4\pi^2} \tag{13}$$

and $\gamma = 5$. The feedback gain matrix of the controller is:

$$\begin{bmatrix} -210.24 & -156.47 & -1250 \\ 17.335 & 12.311 & 126.49 \\ -198.80 & -195.59 & -1561.7 \end{bmatrix} \tag{14}$$

Time Delay Control Time Delay Control is a variety of Model Reference Control. Such control aims to produce dynamic characteristics in the system being controlled that are close to those desired. In actual fact, we constructed a reference model having the desired dynamic characteristics, and designed a controller intended to reduce the difference between the reference model and the actual system to zero. A special feature of this control theory is that, without using a plant model, it controls dynamic characteristics and unexpected disturbance to within the limits of the model, by using data from the very recent past to deduce very close approximations. In designing this controller, the reference model used was:

$$\dot{\mathbf{X}} = \mathbf{A_m X} + \mathbf{B_m r} \quad (15)$$

$$\mathbf{A_m} = \begin{bmatrix} 0 & 1 \\ -1200 & 40 \end{bmatrix}, \mathbf{B_m} = \begin{bmatrix} 0 \\ 1200 \end{bmatrix}$$

Consequently, controller u(t) was

$$u(t) = \frac{1}{\beta}[\beta u(t-L) - \dot{x}_2(t-L)40x_2(t) - 1200X_1(t) + 1200r(t)] \quad (16)$$

where, $x_1(t)$: Speed of control object, $x_2(t)$: Displacement of control object, β : Input gain = -0.52/L, $u(t)$: Input to the plant, $r(t)$: Input to the reference model, L: Sampling time

Sliding Mode Control Sliding Mode Control is a control theory based on Variable Structure System theory. To produce the desired dynamic characteristics, it combines the different dynamic characteristics resulting from differences in control output, switching between the different characteristics according to a particular switching principle. The major feature of Sliding Mode Control is that is concentrates all loci on a single switching plane in the phase plane. Moreover, by taking into account the difference of the incline of the switching plane and the incline of the system's eigen vector, this control theory is able to construct a control system that is not affected by parameter variation or disturbance. We designed the controller for saddle type and vortex type characteristics. The sliding plane, s, calculated using the Lyapunouv Stabilization Theorem, is

$$s = 40x + \dot{x} \quad (17)$$

and control output, u, is

$$sx > 0 : u = 5.0x + 900\dot{x}$$
$$sx < 0 : u = 5.0x - 900\dot{x} \quad (18)$$

EVALUATION TESTS

Evaluation Methods In evaluating the characteristics of the control theories, the aspects given in the table below were used.

TABLE 1: Evaluation Methods of Characteristics

Characteristics	Evaluation aspect
Steady-state characteristics	Step response
Response speed	Impulse response
Stability	Open loop transfer function
Robustness	Complimentary sensitivity function
Disturbance suppression effect	Sensitivity function
Rigidity	Compliance

Steady-State Characteristics

A comparison of step response is shown in Fig. 6. Looking first at the steady-state characteristics up until the step input is actuated (target levitation position: 1.227V), we see that TDC has the most outstanding performance, with levitation occurring at almost the target levitation position. After TDC, the performance ranking in descending order is: $H\infty$,PID, LQG, Sliding Mode. The performance ranking is the same after step input is actuated.

Response Speed Impulses response results are shown in Fig. 7. In the settling time, $H\infty$ had the best performance, followed by PID, LQG, Sliding Mode and TDC in that order. TDC and Sliding Mode response was shaky. $H\infty$ showed good responseness , but had a small amount of overshoot.

Stability Bode plots for the open loop transfer function is shown in Fig. 8. $H\infty$ and PID have wide phase and gain margins, and consequently excellent stability.

Robustness Bode plots for the closed loop transfer function is shown in Fig. 9. LQG had the best robustness when spillover occurred in the higher order vibration mode. This is thought to be because the controller designed according to the LQG theory cuts the higher order vibration mode in the same way that it cuts noise. The next best control theories in terms of robustness were PID and $H\infty$ In the case of PID, this is because the PID controller uses incomplete differentials to deal with excessive increase in gain in the high frequency range. In the case of $H\infty$ it is because in the high frequency range this controller increases gain of weight function relative to complementary sensitivity function. Controller with poor robustness were TDC and Sliding Mode. In the case of TDC, this was because the controller contains

a complete integral element, a complete differential element and a proportional element. This complete differential element cause the high frequency range gain to increase, which induces the higher flexible mode vibration.

Disturbance Suppression Effect

Measurement results of sensitivity function are shown in Fig. 10. Controller with good disturbance suppression effect in the region of 1Hz were PID, LQG, Sliding Mode and TDC. With Sliding Mode and TDC, disturbance suppression effect is poor in the region of the rigid body mode, and in particular the system by Sliding Mode controller became unstable. Control theories with good disturbance suppression even in the region of the rigid body mode were $H\infty$ PID and LQG. In the case of $H\infty$ there is a tendency for gain to decrease in the low frequency range. This is because in the low frequency range, this controller increases the gain of weight function relative to sensitivity function.

Rigidity The measurement results of compliance are shown in Fig. 11. $H\infty$ and PID have uniform rigidity across the entire frequency range. With LQG and TDC, rigidity is weak in the region of the rigid body mode, but rigidity in TDC shows a tendency to increase with lower frequency. The compliance of Sliding Mode Controller could not be measured because the system became unstable during measurement.

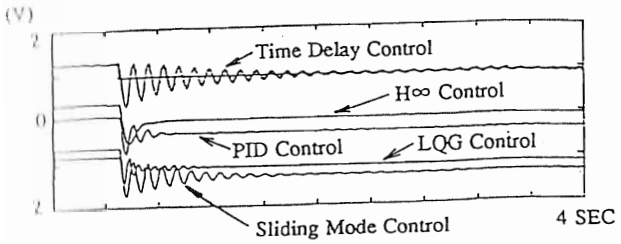

FIGURE 6: Time history of step response

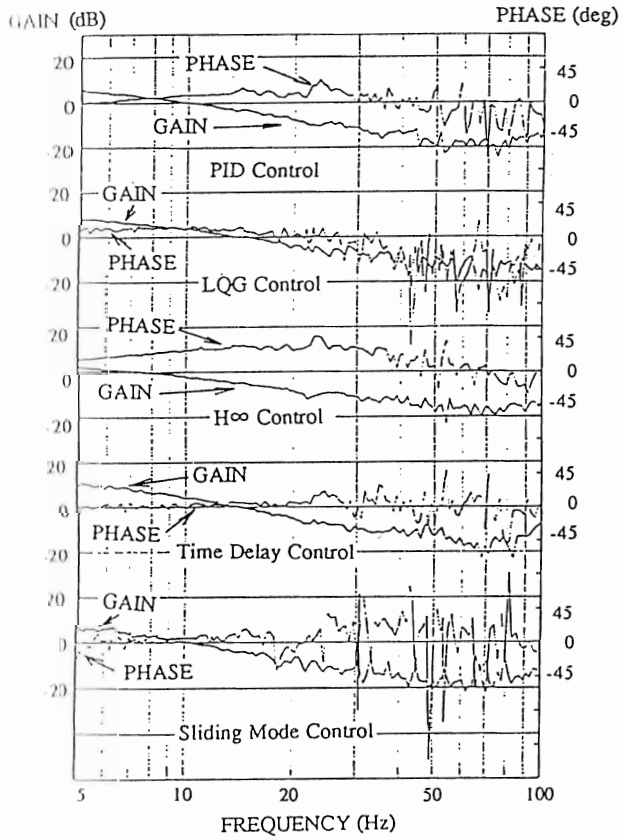

FIGURE 7: Time history of impulse response

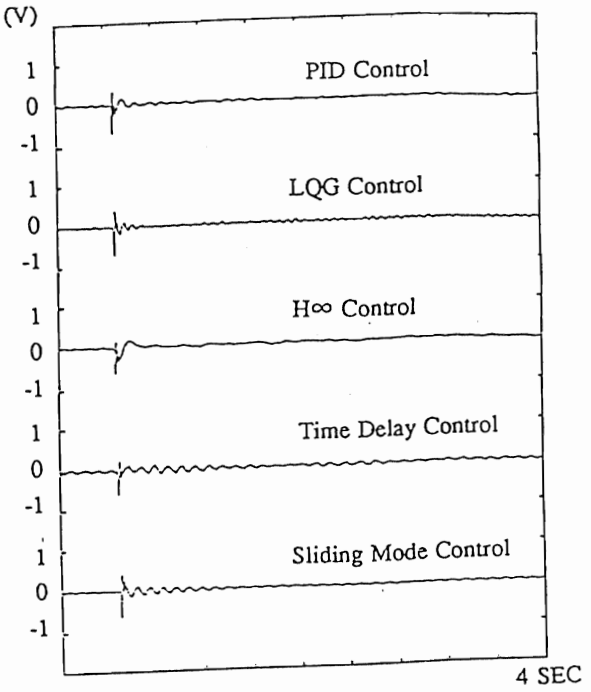

FIGURE 8: Bode diagram of open-loop system

CONCLUSIONS

The following conclusions can be drawn from a consideration of the controller characteristics evaluated in the electromagnetic levitation tests.

(1) PID control requires a high order of controller performance, but an excellent controller can be designed using existing know-how.

(2) Using the LQG control theory, a controller with excellent disturbance suppression effect and response

speed can be designed and can be used to suppress oscillation caused by spillover in the higher vibration mode.

(3) Using the $H\infty$ control theory, a controller with excellent disturbance suppression effect, robustness and stability can be designed. However, this theory uses weight function , so designing a controller using enlarged plant allowing for disturbance and error would be time-consuming.

(4) Using the Time Delay Control theory , a controller is simple to design. This theory provides high rigidity . However, spillover oscillation of higher vibration mode is prone to occur .

(5) Using Sliding Mode Control, a controller with excellent disturbance suppression effect in the low frequency range was obtained. Moreover, using the Lyapunov Stabilization Theorem makes the controller comparatively easy to design.

REFERENCES

(1) Nakano,M.,Mita,T., Basic Control Theory , Syoukou-dou (in Japanese) (1982)

(2) Masubuti,M., System control , Korona-sya (in Japanese) (1987)

(3) SICE Lecture Textbook , Introduction to Modern Control Theory , SICE (in Japanese) (1991)

(4) Harasima, F., Sliding Mode control , Computrol No.13 (1986)

(5) Youcef-Toumi,K., A Time Delay Controller for system with Unknown Dynamics Proc.American Control Conf.(1987)

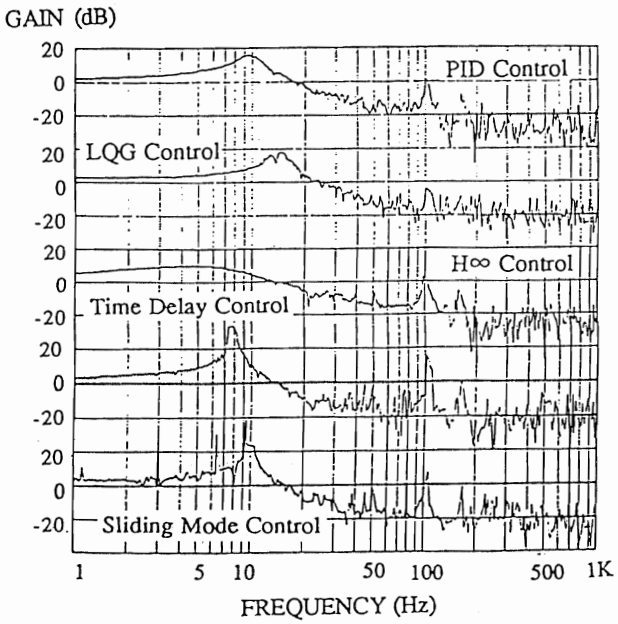

FIGURE 9: Bode diagram of closed-loop system

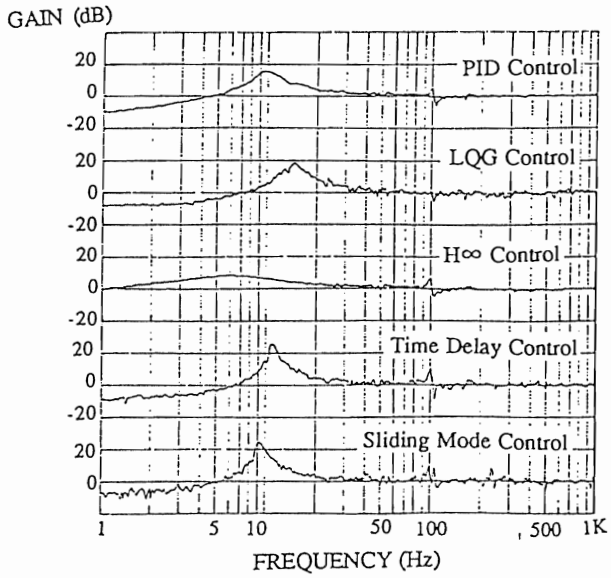

FIGURE 10: Bode diagram of sensitivity function

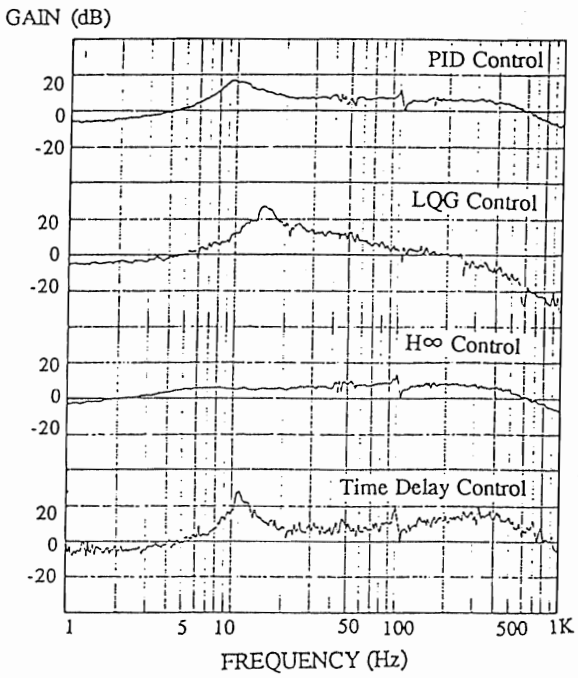

FIGURE 11: Bode diagram of compliance of system